Aeroacoustic Results from Common Research Model Testing and Analysis

David Lockard

Advanced Air Transport Technology (AATT) Project

NASA Acoustics TWG meeting, April 12-13, 2022

2022 Aeroacoustic Conference Papers

Development of Slat Gap and Slat Cove Filler Treatments for Noise Reduction Assessment on the High Lift Common Research Model in the NASA LaRC 14x22

Turner, T. L., Mulvaney, J. W., Allen, A. R., Brynildsen, S. E., and Lockard, D. P.

On the Alleviation of Background Noise for the High-Lift Common Research Model Aeroacoustics Test

Hutcheson F. V., Lockard D. P., Bahr, C. J., Stead D. J.

Accounting for the Influence of Decorrelation in Microphone Phased Array Deconvolution Methods

Bahr, C. J.

Phased Array Characterization of Slat Noise Radiation from the High-Lift Common Research Model

Humphreys Jr., W. M., Lockard, D. P. and Bahr, C. J.

Aeroacoustic Simulations of the High-Lift Common Research Model and Validation with Experiment

Lockard, D. P., Choudhari, M. M., and Vatsa, V. N.

2022 AIAA/CEAS Aeroacoustics Conference, Southampton, U.K., June 14-17, 2022

Development of SGF & SCF Treatments for Noise Reduction Assessment on the CRM-HL

Travis Turner, John Mulvaney, David Lockard,
Albert Allen, Scott Brynildsen

Background/Motivation for CRM-QHL

Approach

- **2D representation of flight geometry**
- **Parametric study of SGF & SCF**
- **Validated computational models**
- **Motivated CRM-HL treatments & test in the 14- by 22-Foot Subsonic Tunnel (14x22)**

Slat Gap Filler (SGF)

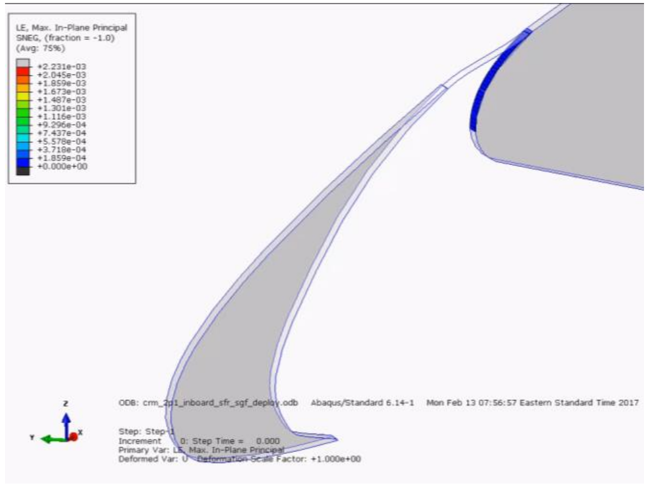

Slat Cover Filler (SCF)

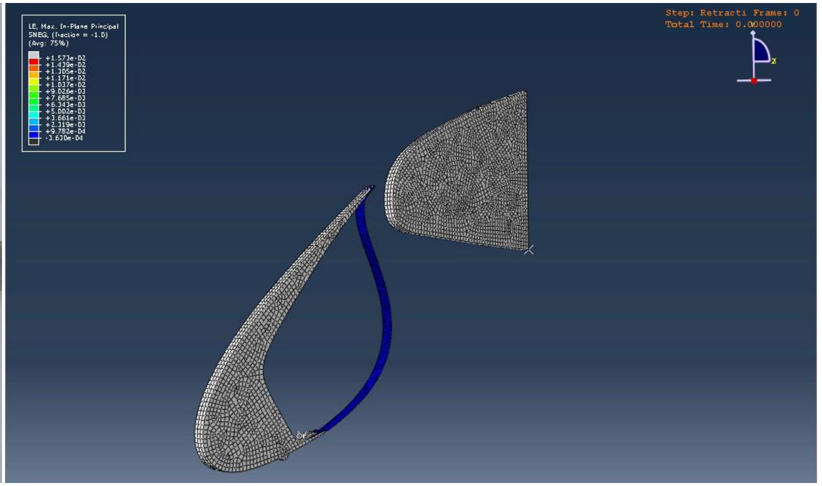

CRM-QHL Treatment Concepts

SGF on Full-Span Slat
Viewed from Outboard & Above

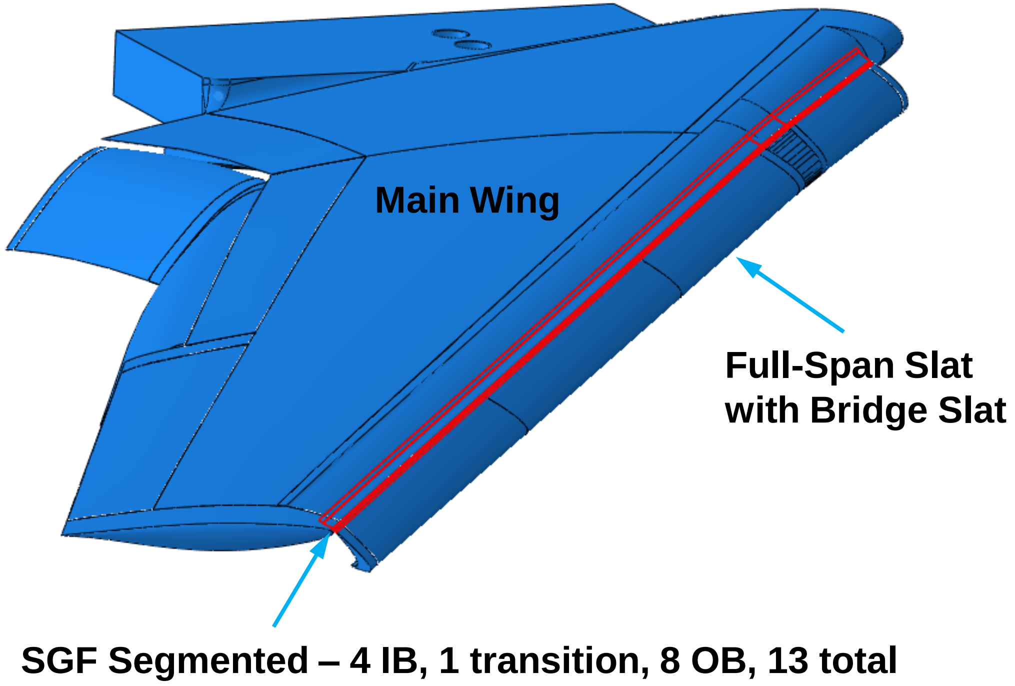

SCF on OB Slat
Viewed from Outboard & Below

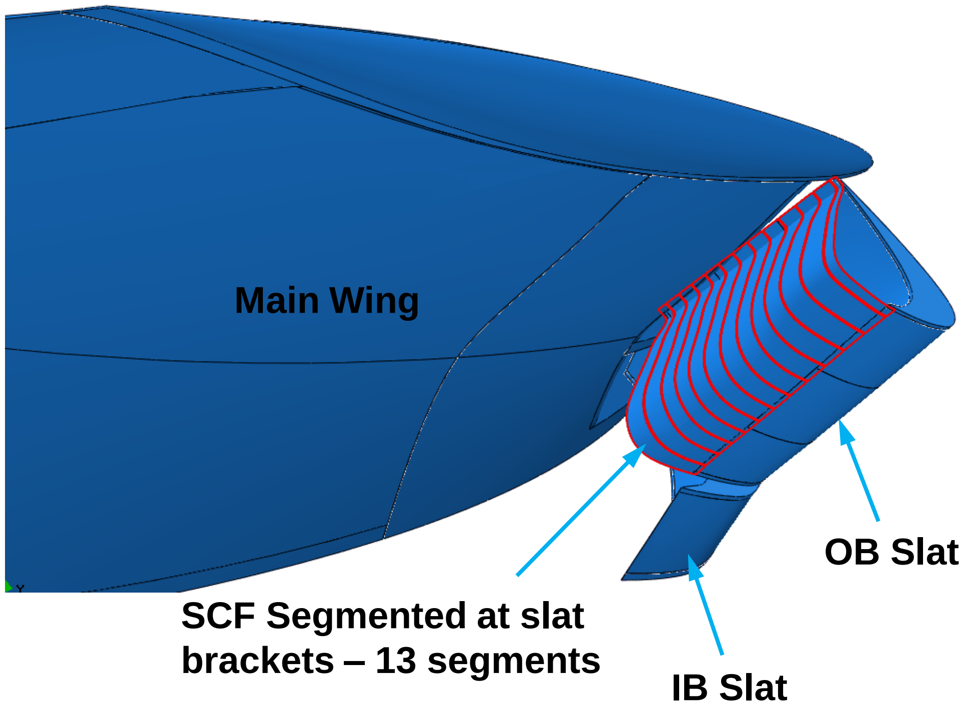

SGF and SCF concepts shown motivated by previous work

Challenges

- **3D effects – sweep, taper, spanwise irregularities**
- **Large change in thickness/chord ratio of slat with spanwise location**
- **Model scale – treatments dynamically scaled with compromise on model integration**

CRM-QHL SGF & SCF Treatment Design

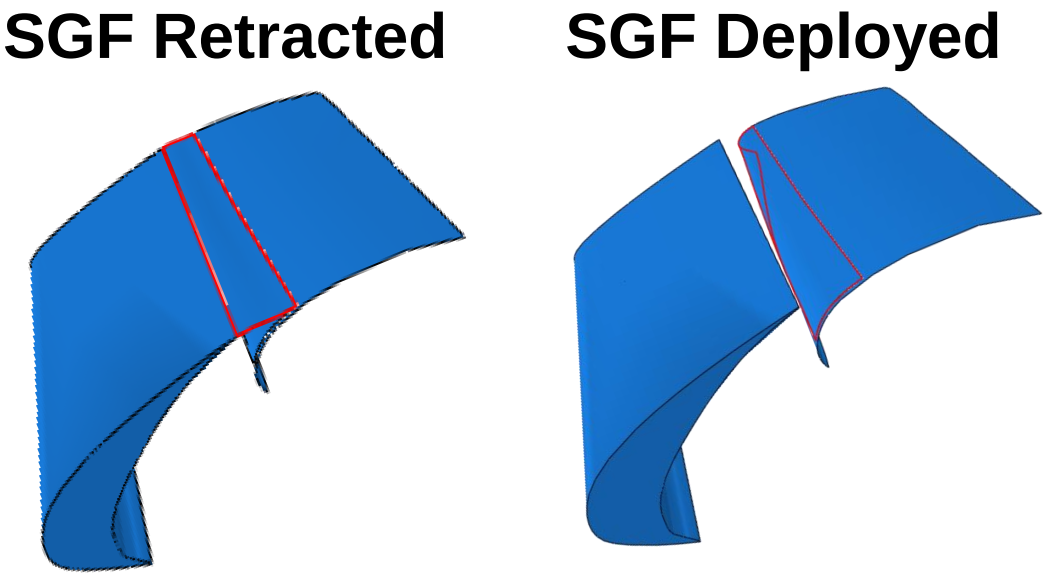

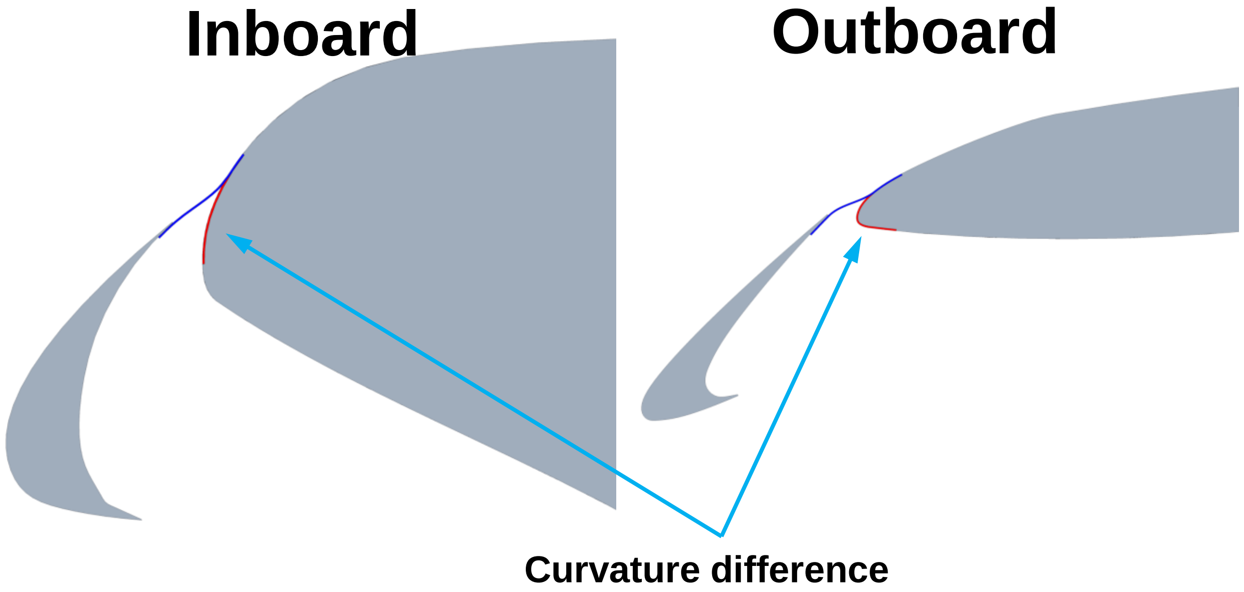

- **Concepts developed for sweep/taper**
- **CFD exposed new parametric space for SGF**
- **Various SGF implementations studied in 14x22**
- **SGF options offer similar aeroacoustic performance**

CRM-QHL SGF & SCF Integration & Assembly

SGF Treatment – Section at Inboard Slat

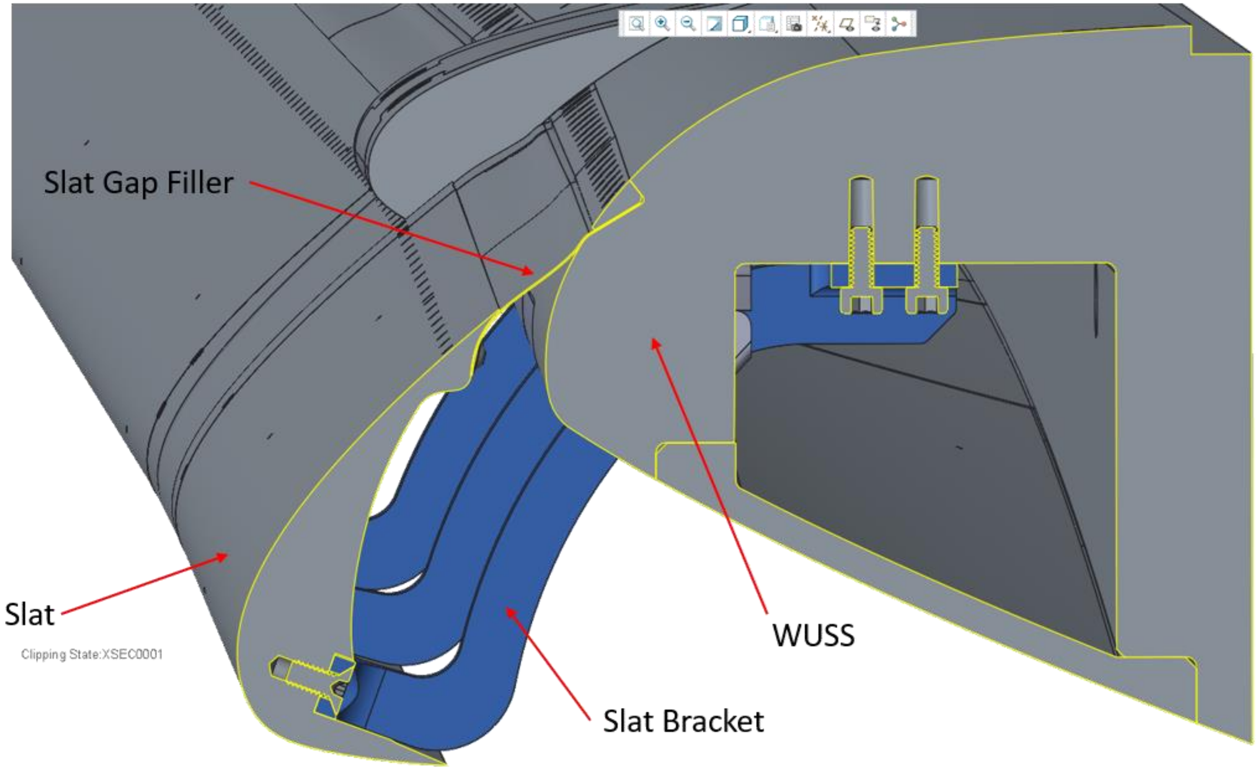

SCF Treatment – Section at Outboard Slat

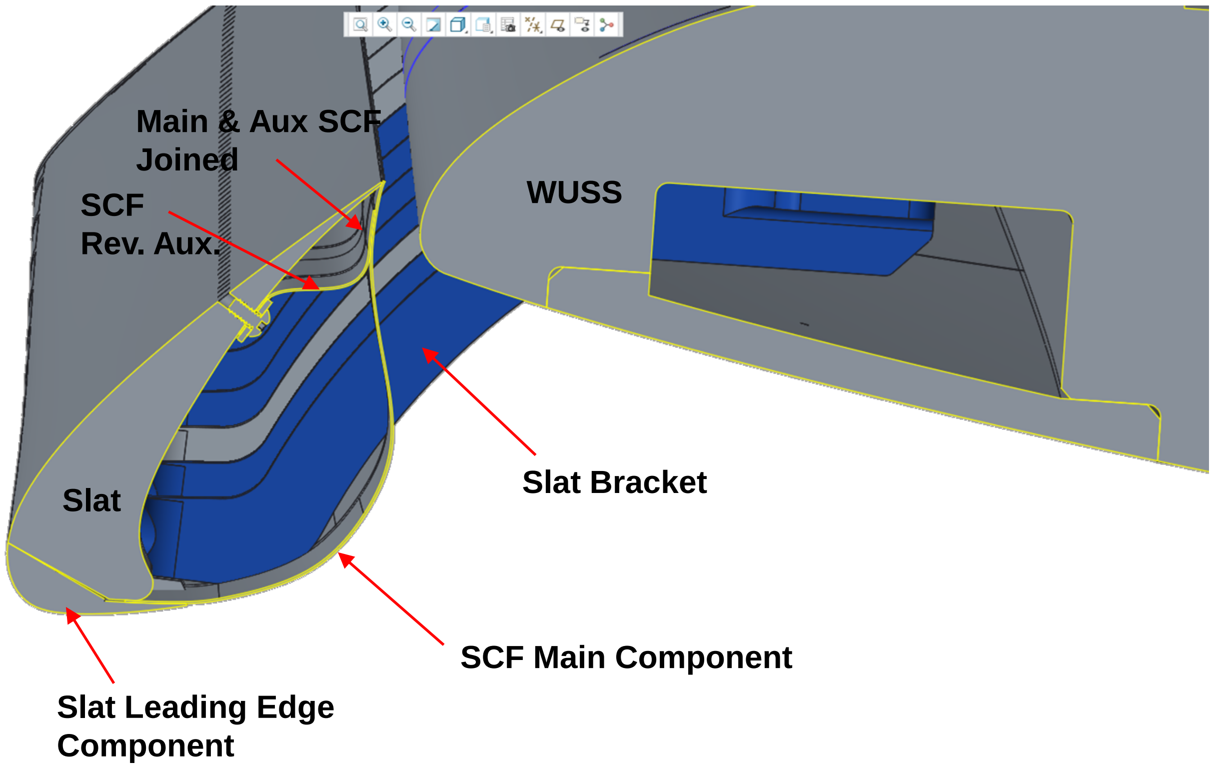

- Fasteners employed for fail-safety
- One of three SGF integration variants shown – all performed similarly
- Treatments sized to steady aero-load & informed by FSI analysis
- Post-test completion of FSI and dimensional analysis indicates overdesign

FSI Assessment of CRM-HL SGF Treatment

CRM-HL Semispan Model w/ Notional FSI Subdomain

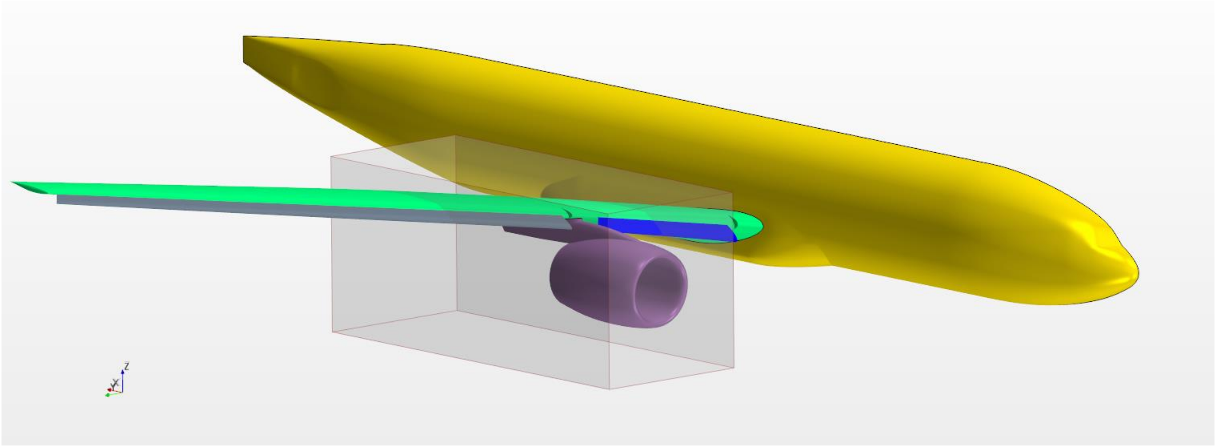

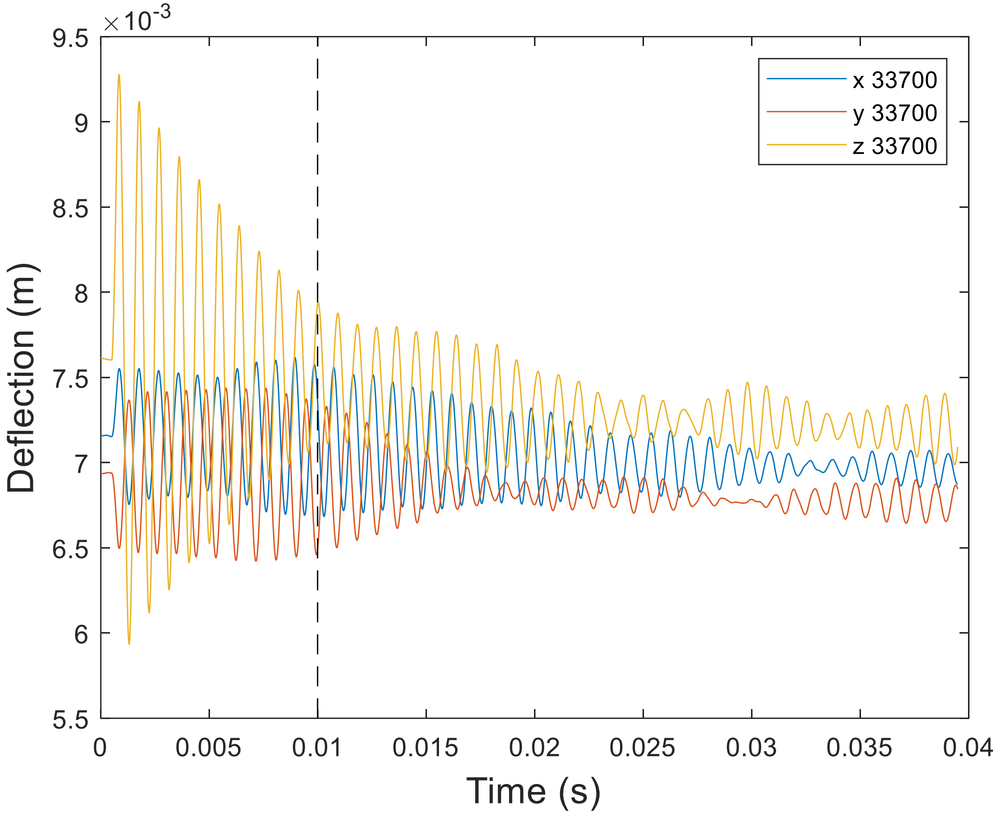

Objective
Assess fluid structure interaction (FSI) behavior of SGF & SCF treatments to be tested on the 10% CRM-HL in the NASA LaRC 14x22

Approach – Collaboration with ATA Engineering
- **Performed FSI analysis via sub-domain FEM and CFD grid**

Outcome
- **2D & 3D assessment of SGF show stable response to 4x q**
- **FUN3D-Abaqus FSI computational framework developed**

Fully Coupled Aeroelastic Stability Analysis of Adaptive Shape Memory Alloy Structural Technologies for Airframe Noise Reduction
Michael R. Nucci, et al., to be presented at the 2022 AIAA AVIATION Meeting.

National Aeronautics and
Space Administration

On the Alleviation of Background Noise for the High-Lift Common Research Model Aeroacoustic Test

Florence Hutcheson, David Lockard and Dan Stead

14x22 Test Section at Start of Test

- Prior to the High-Lift Common Research Model (CRM-HL) test entry, modifications were made to the test section floor acoustic treatment, as well as to the collector and diffuser.

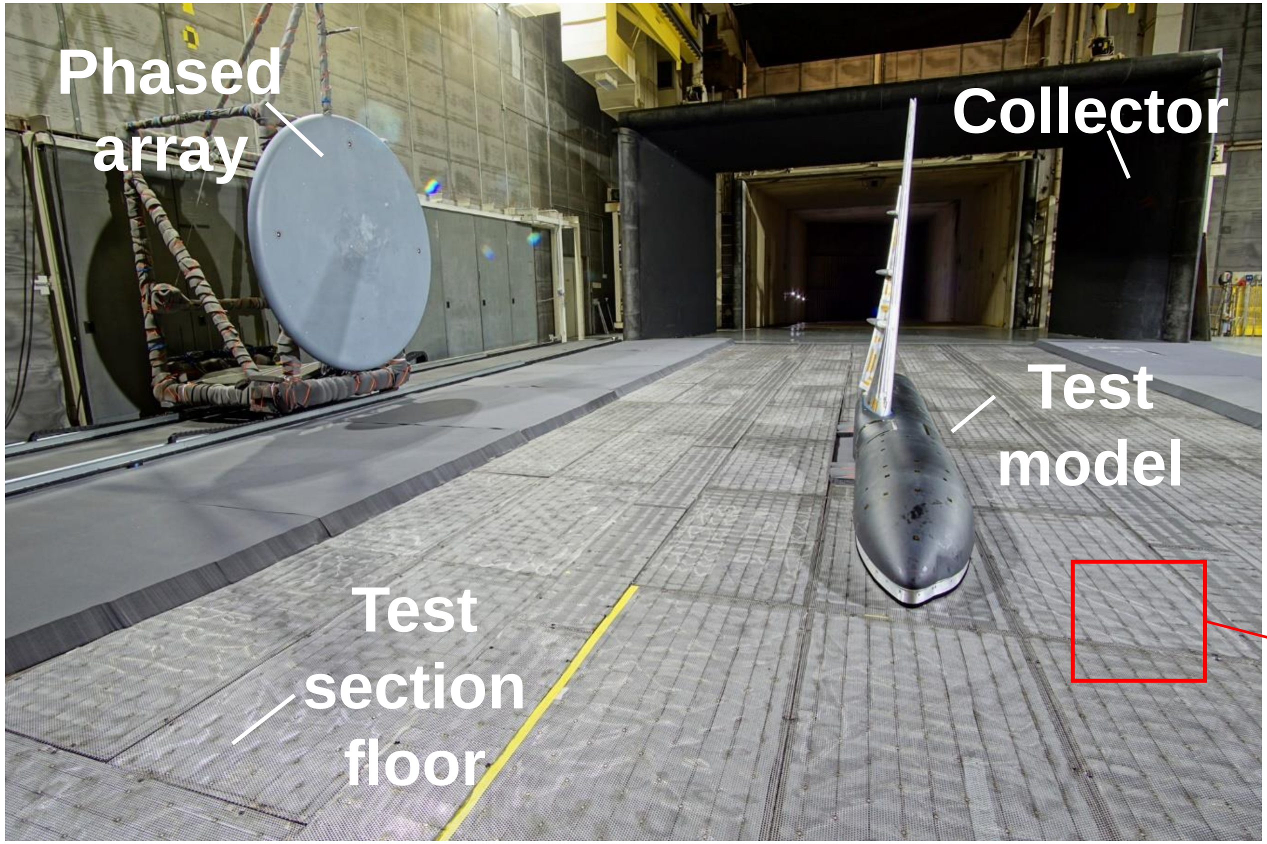

14x22 test section at the beginning of CRM-HL test

- The solid leading edges of the collector and diffuser were replaced with acoustically treated surfaces
- Perforated panels were installed on top of the floor foam filled baskets (without a screen cover fused to it due to lead time and cost).

Noise Map at Start of Test – Mach 0.16, AOA 0°

Test model in a “low noise” configuration

Conventional Beamforming

$f_{1/12th}$ = 12.5 kHz

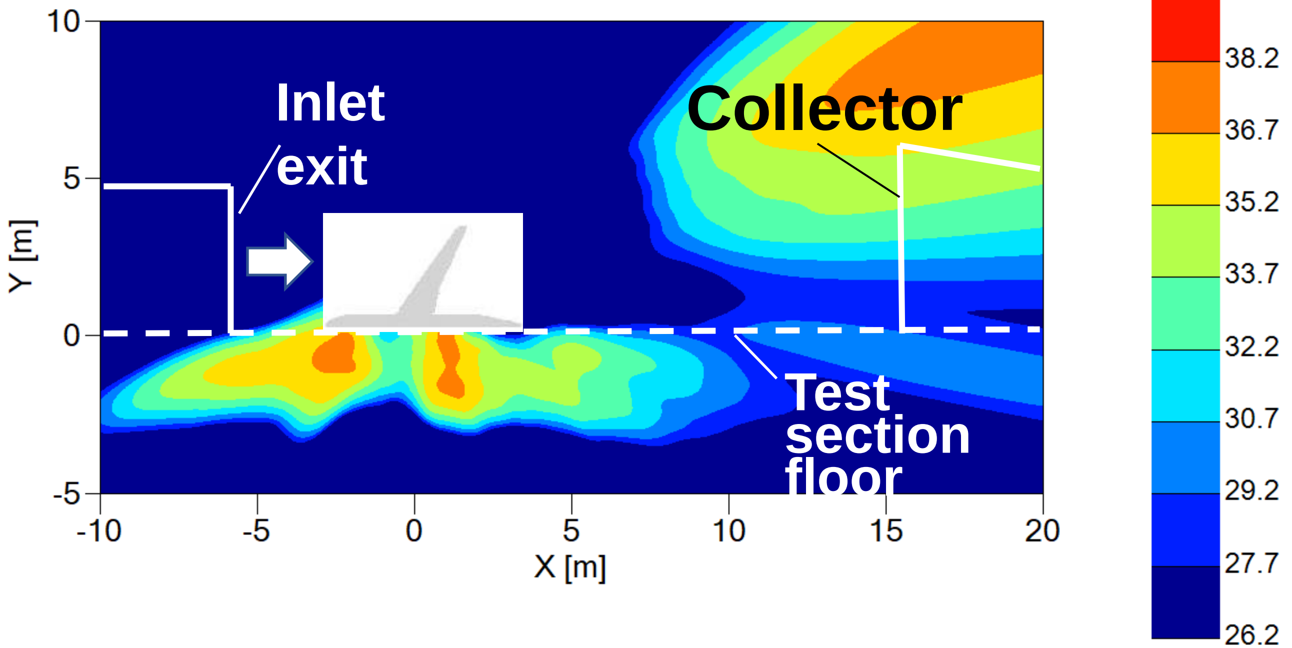

- **Initial measurements quickly revealed noise spectral levels higher than they should be, as well as extraneous noise around the test model near floor junction and above collector.**

Felt Treatment on Collector / Diffuser & Floor

- 1/8" thick polyester felt with very thin (.003") adhesive film and of 3 different densities (8, 18 and 32 oz./yd^2) was used to treat the test section:

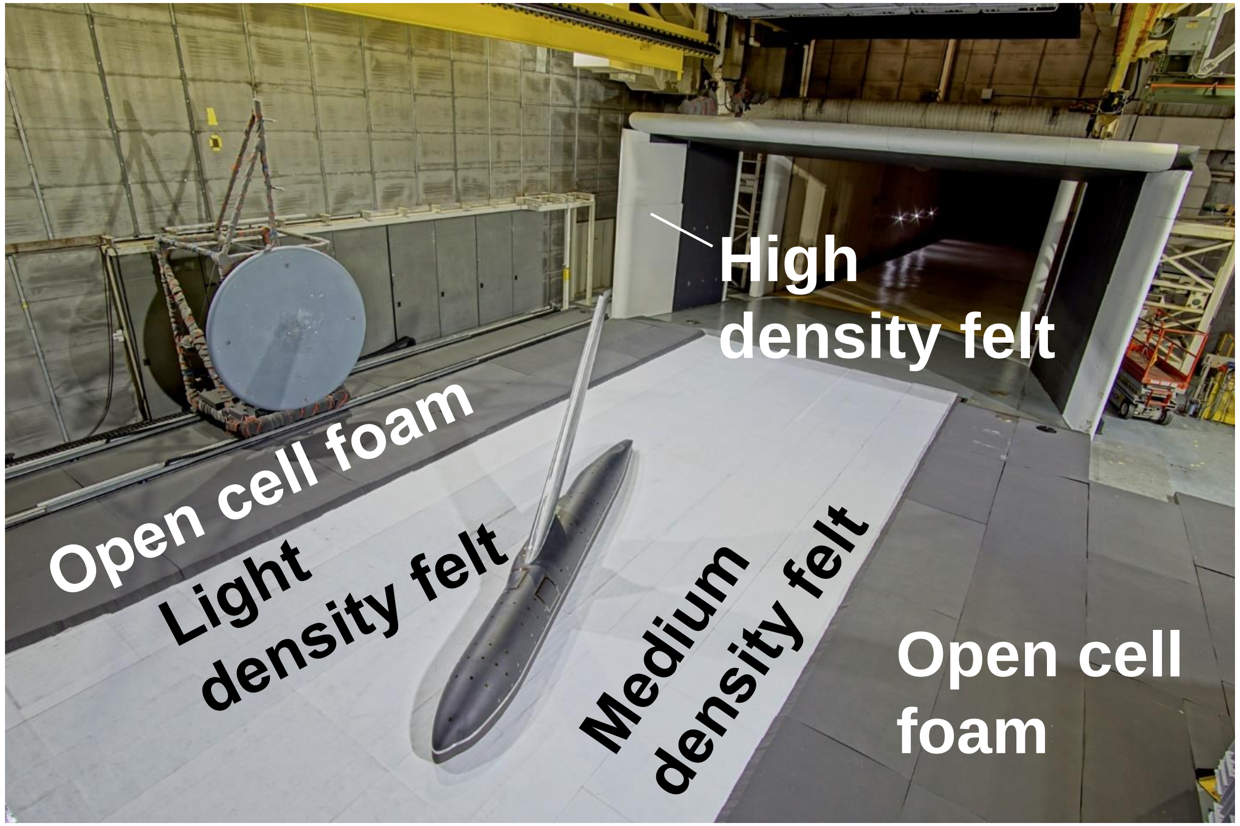

- High density felt on the collector and diffuser to dampen the noise resulting from the strong interaction of the test section shear layer with leading edge surfaces.
- Light & medium density felt on test section floor to alleviate scrubbing noise from the perforated panels.

Felt on Collector / Diffuser and Floor

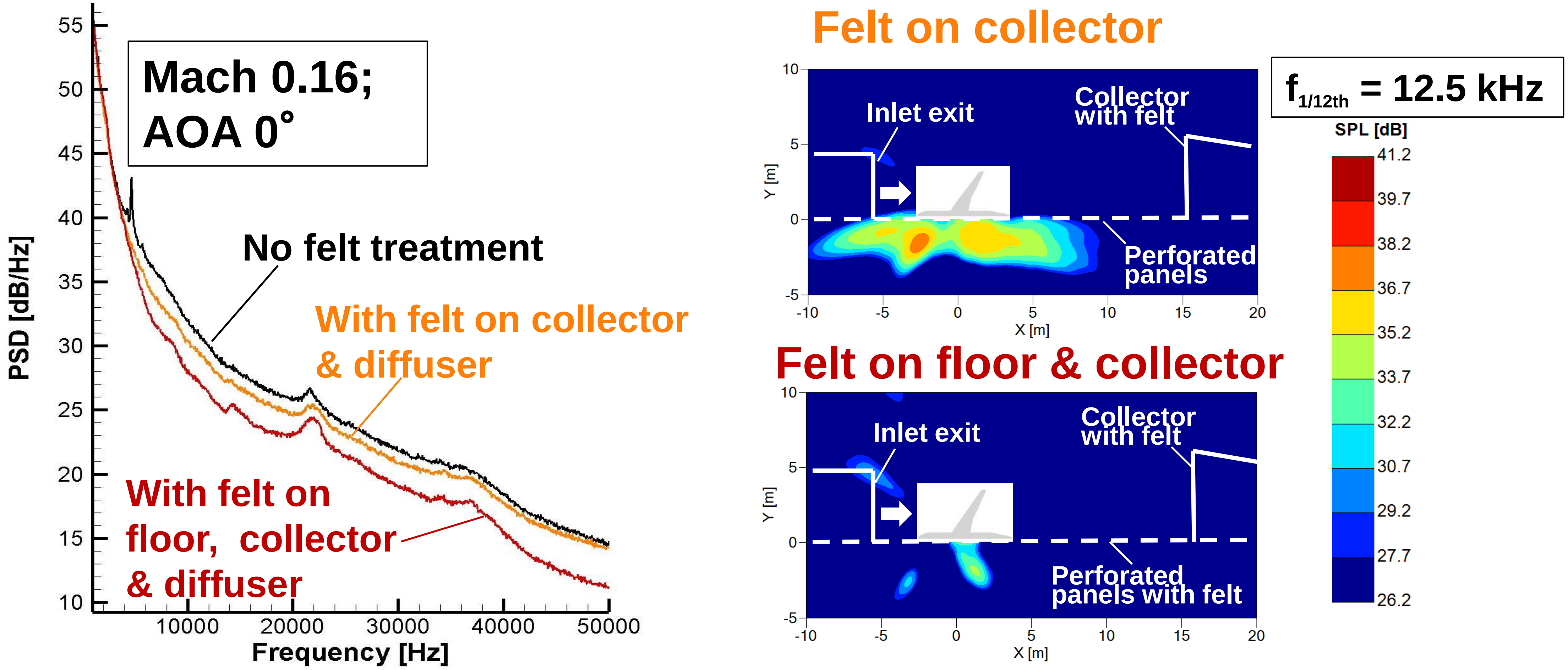

- Noise eliminated around the model junction with the floor and in the collector.
- Noise spectral levels significantly reduced over broad frequency range.

Scrubbing Noise Measurements from floor basket top

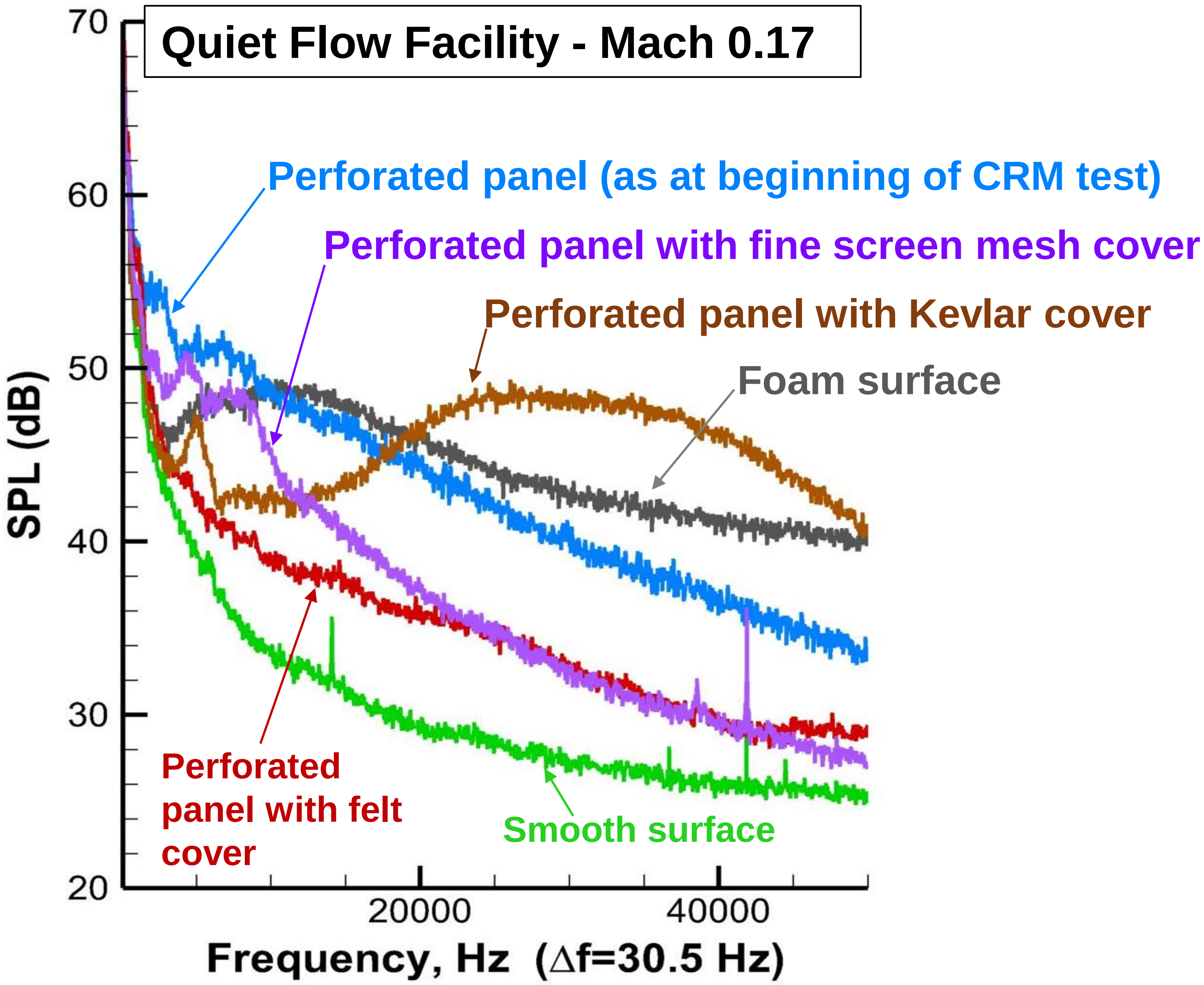

- **Scrubbing noise measurements from different basket top covers (felt, fine screen mesh and Kevlar) were performed in the Quiet Flow Facility following the HL-CRM test.**

- **Scrubbing noise from the felt covering was found to be significantly lower than that from other material tested.**

Summary

- **The felt treatment was a stop-gap solution that sufficiently resolved the elevated background noise problem in the 14x22 for the HL-CRM test.**

- **However, although the felt covering has significantly lower scrubbing noise levels than the legacy foam baskets (foam covered by a grid), each additional layer of material applied over the foam (i.e., perforated panel and felt) affects the floor acoustic absorption.**

Accounting for the Influence of Decorrelation in Microphone Phased Array Deconvolution Methods

Christopher J. Bahr

Phased Arrays and Decorrelation

- Propagation through turbulence – randomization of acoustic signal
  - Degrades coherence of cross spectra
  - Blurs beamforming and deconvolution source maps constructed from phased array data
- Modeling the effect can improve array output
  - Model dependence
    - Turbulence length scale
    - Variance of index of refraction (velocity fluctuations in controlled wind tunnel tests)
    - Propagation distance through turbulence, X_L
    - Separation distance of microphones, ρ
  - Model construction
    - Measure all parameters directly
    - Fit turbulence length scale/variance using a reference source

Initial Model (2021)

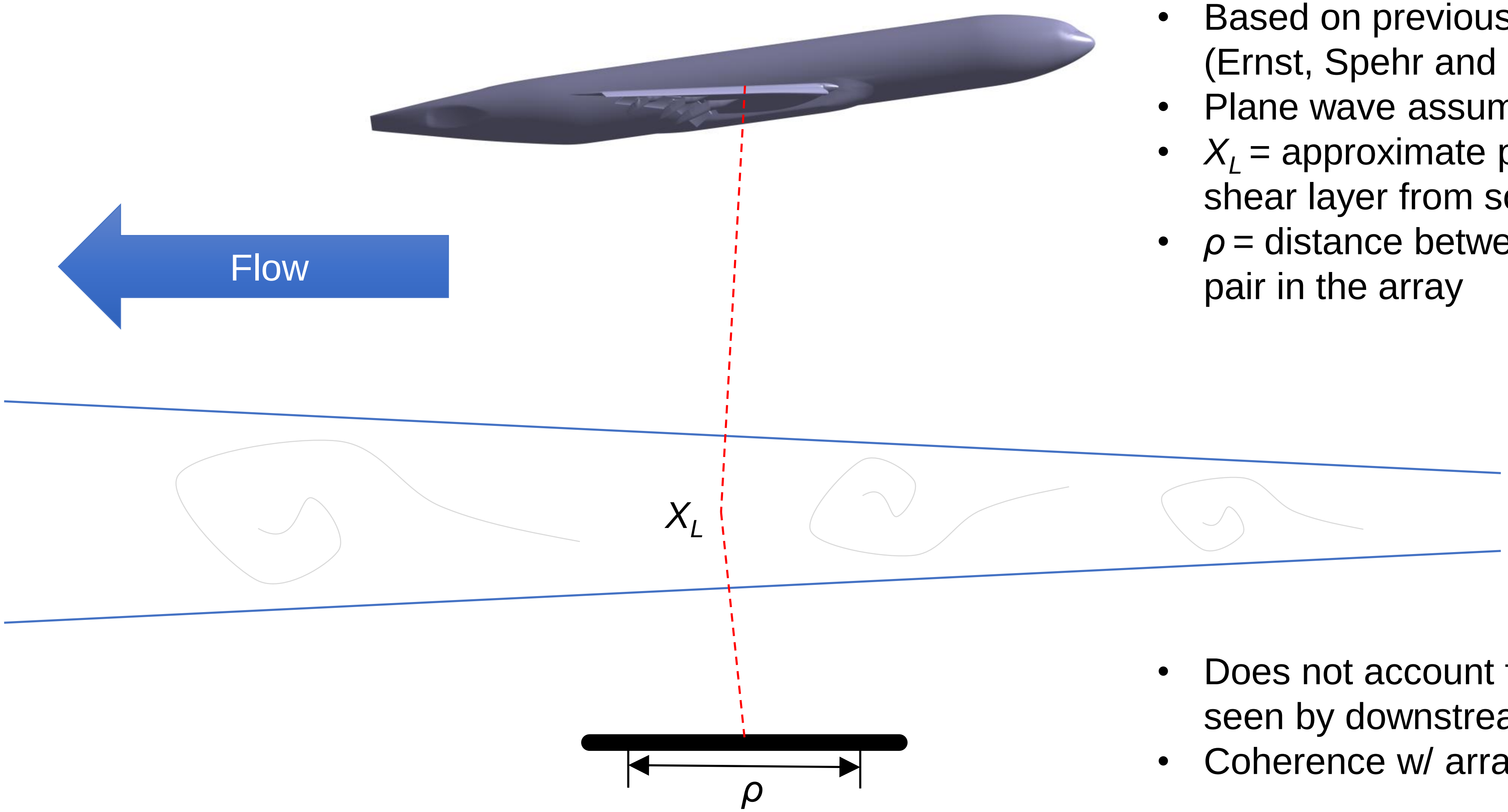

- Based on previous wind tunnel studies (Ernst, Spehr and Berkefeld, 2015)
- Plane wave assumption
- X_L = approximate path length through shear layer from source to array center
- ρ = distance between any microphone pair in the array

- Does not account for thicker shear layer seen by downstream microphone pairs
- Coherence w/ array center is axisymmetric

Ernst, D., Spehr, C., and Berkefeld, T., "Decorrelation of Acoustic Wave Propagation through the Shear Layer in Open Jet Wind Tunnel," *21st AIAA/CEAS Aeroacoustics Conference*, AIAA 2015-2976, Dallas, Texas, 22 – 26 June 2015.

Array Processing

- Conventional frequency-domain beamforming (CBF) coupled with DAMAS deconvolution.
- DAMAS algorithm was modifie to correct for propagation path randomization through shear layer.
- Correction incorporates a Mutual Coherence Function (MCF) into DAMAS propagation model (referred to as MCF-DAMAS).
- Source integration performed on MCF-DAMAS spectral levels to compute 1/12th-octave SPL integrated spectra.

Reference: Bahr, C.J., "Accounting for the Influence of Decorrelation in Microphone Phase Array Deconvolution Methods", 2022 AIAA/CEAS Aeroacoustics Conference, Southampton, U.K., 2022.

Traditional DAMAS

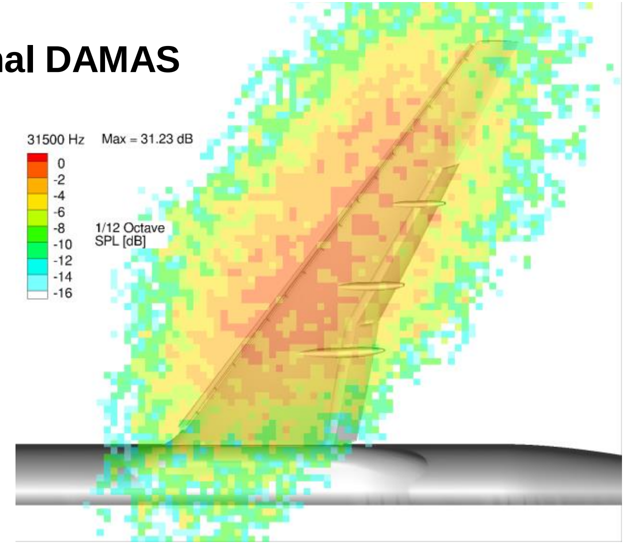

MCF-DAMAS

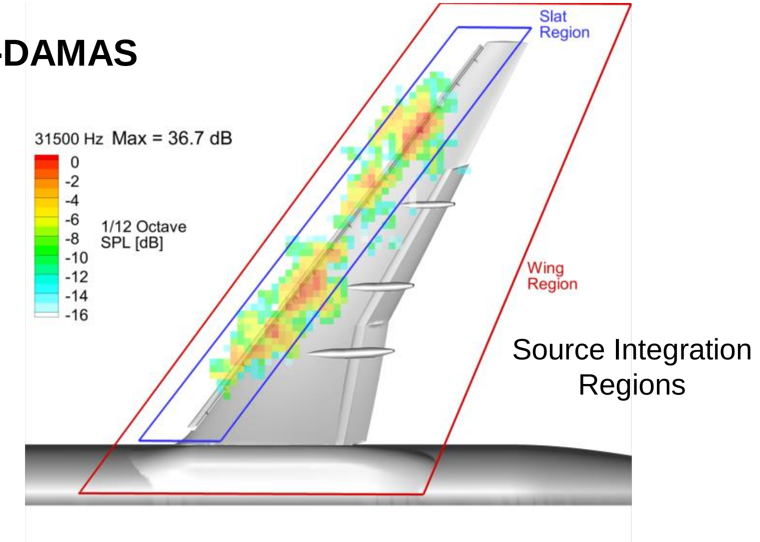

31.5 kHz

Model Update (2022)

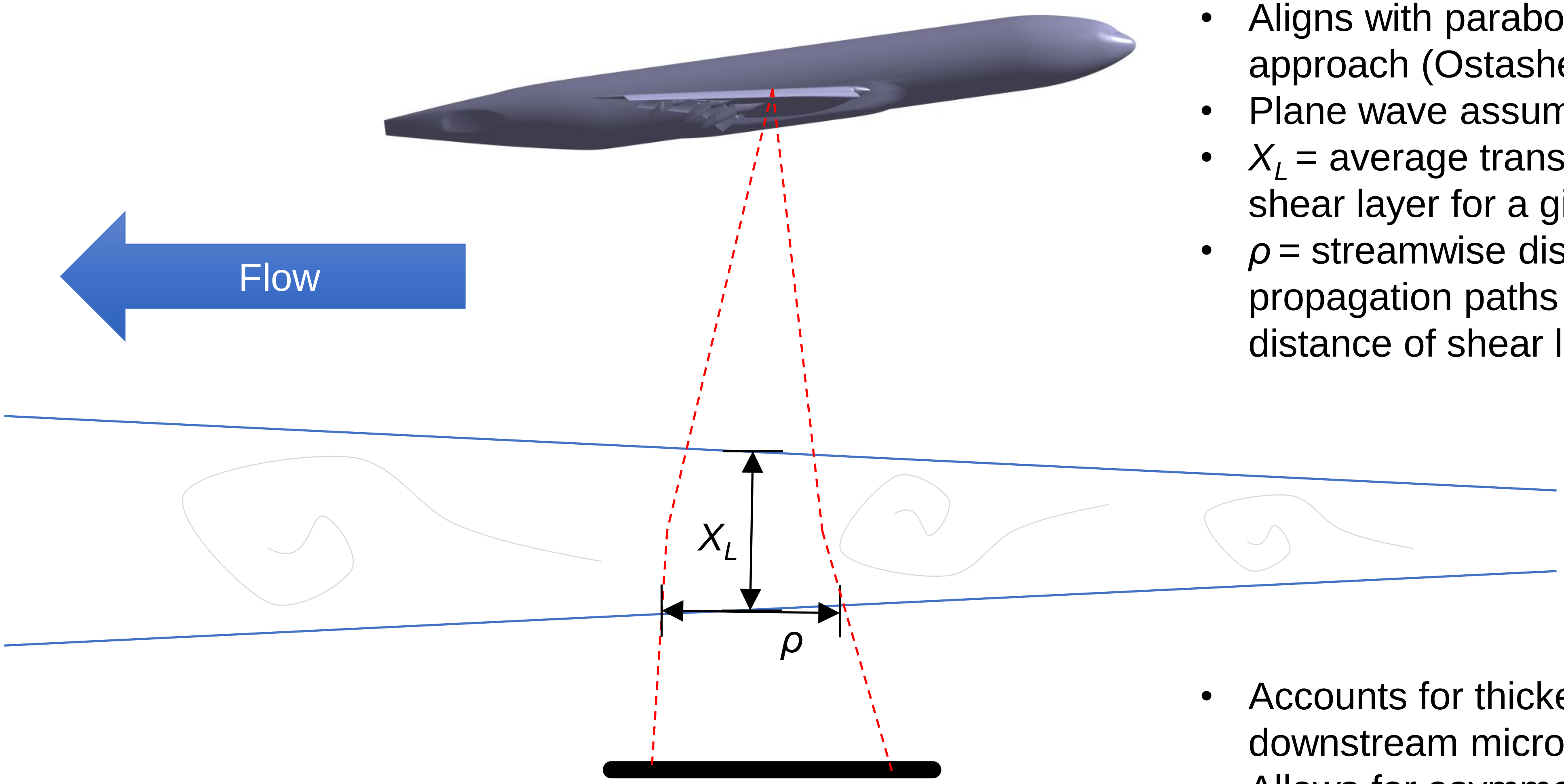

- Aligns with parabolic/layered media approach (Ostashev & Wilson 2016)
- Plane wave assumption
- X_L = average transverse distance through shear layer for a given microphone pair
- ρ = streamwise distance between propagation paths at average transverse distance of shear layer exit

- Accounts for thicker shear layer seen by downstream microphone pairs
- Allows for asymmetric coherence distributions when referencing the array center

Ostashev, V., and Wilson, D., "Line-of-sight sound propagation in a random moving medium," in *Acoustics in Moving Inhomogeneous Media*, 2nd ed., CRC Press, 2016.

Phased Array Characterization of Slat Noise Radiation from the CRM-HL Research Model

National Aeronautics and Space Administration

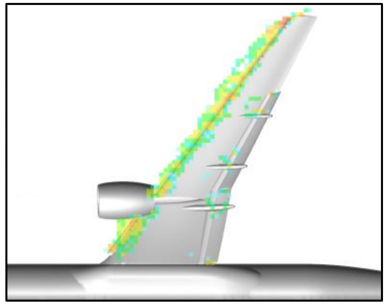

William M. Humphreys Jr., David P. Lockard, and Christopher J. Bahr

NASA acoustics
Technology for a quieter world

14- by 22-foot Subsonic Tunnel Traversing Array

- Total of 97 flush-mounted B&K 4938 pressure microphones, arranged in 16 array arms.
- Maximum array aperture of 2 meters, yielding a solid collecting angle of 21.1° from array face to tunnel centerline.
- Mounted on 13.4-meter linear traversing rail on “south” side of test section, allowing viewing of pressure side of model at flyover directivity angles spanning 56° to 120°.

Sampling rate – 196.608 Hz
Bandpass filtered from 1 - 60 kHz
Acquisition window – 35 seconds

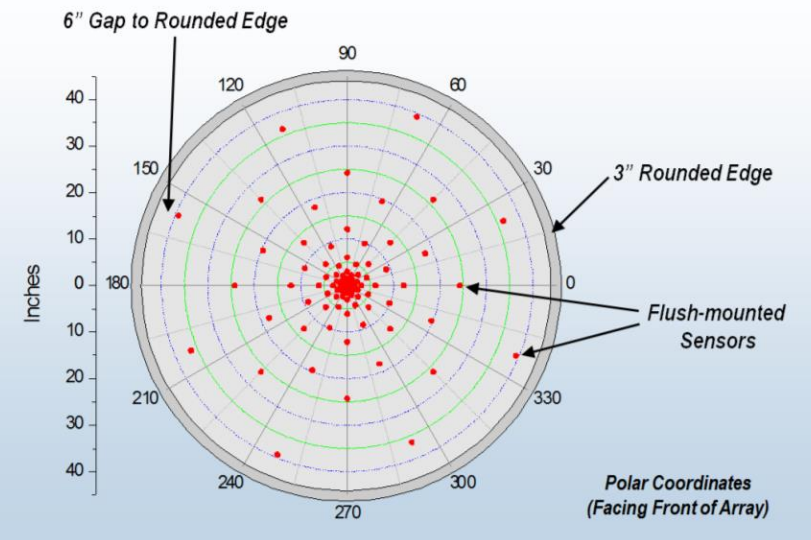

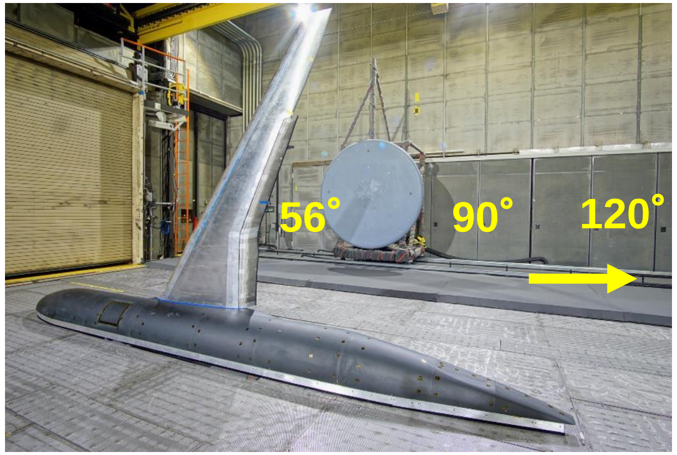

Model Configurations Measured with Array

Configuration #	Full-span Slat (FSS)	Part-span Slat (PSS)	Slat Gap Filler (SGF)	Nacelle	Main Landing Gear (MLG)
1	X				
2	X		X		
3	X		X		X
4		X		X	
5		X		X	X
6		X	X	X	
7		X	X	X	X

Shown Here

- Two slat configurations tested:
  - Full-span slat where pylon and nacelle were removed and replaced with bridge section
  - Part-span slat with pylon and nacelle in place
- Model geometry included 15 slat brackets
- SGF fabricated out of nickel-titanium shape-memory alloy (SMA)
  (Ref: Turner, AIAA Paper 2015-0730, SciTech 2015)

Baseline Full Span Slat (FSS) – Configuration 1

- At lower frequencies, noise radiation from outer slat region and wing tip dominate.
- At higher frequencies, noise radiation more uniform across slat span.
- Flap noise not a significant contributor to overall noise.

6 kHz

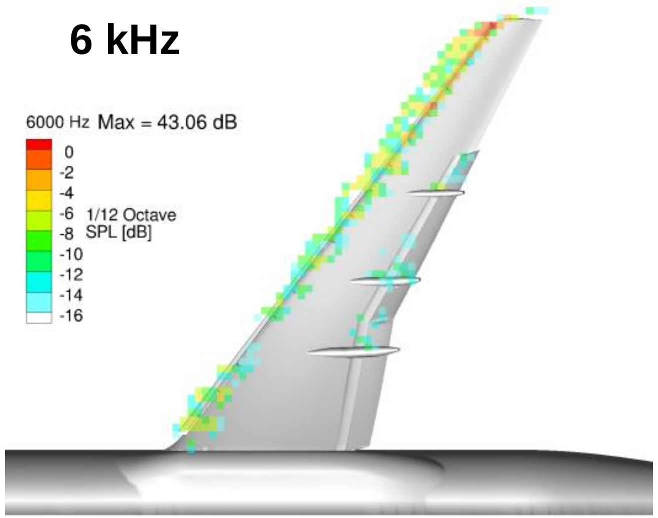

10 kHz

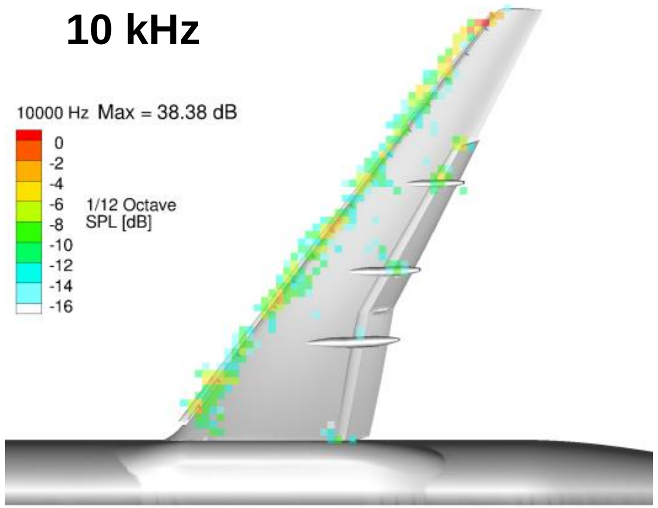

20 kHz

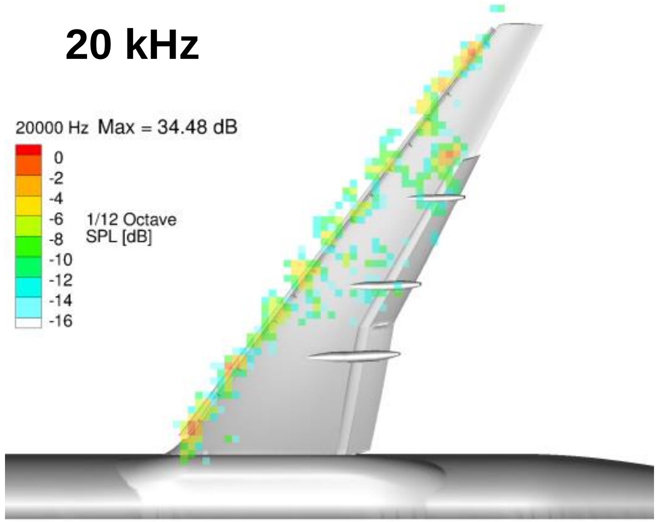

1/12-octave band MCF-DAMAS output, P3903
$\alpha = 8.5°$, $M = 0.16$, $\phi = 90°$

Baseline Full Span Slat (FSS) – Configuration 1

Mach Number Scaling
α = 8.5°, ϕ = 90°

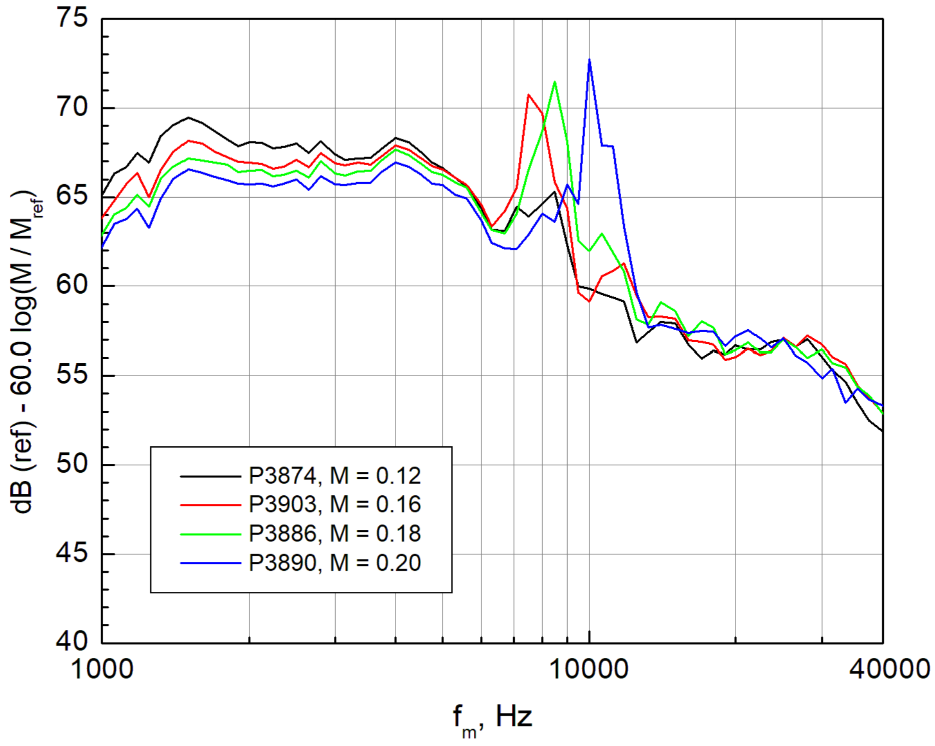

Directivity Scaling
α = 8.5°, M = 0.16

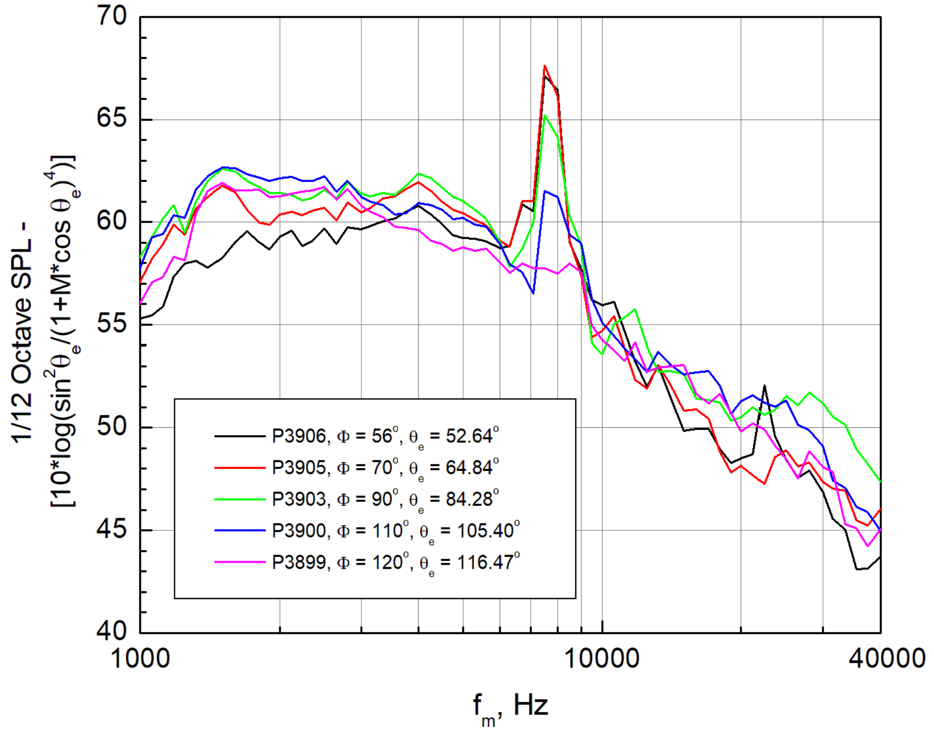

- Mach number scaling confirms a sixth power dependency on flow speed above 15 kHz. (Scaling appears to exhibit a fifth power dependency below 5 kHz.)
- Baseline slat noise acts as a pseudodipole source, confirmed using directivity scaling function above. *(Ref: Mendoza, Int. Journal of Aeroacoustics, 2002)*

Slat Gap Filler FSS – Configuration 2

- Addition of SGF eliminates majority of slat noise via disruption of flow through the gap.
- With reduction of slat noise, flap noise becomes more prominent (but still low-level).

6 kHz

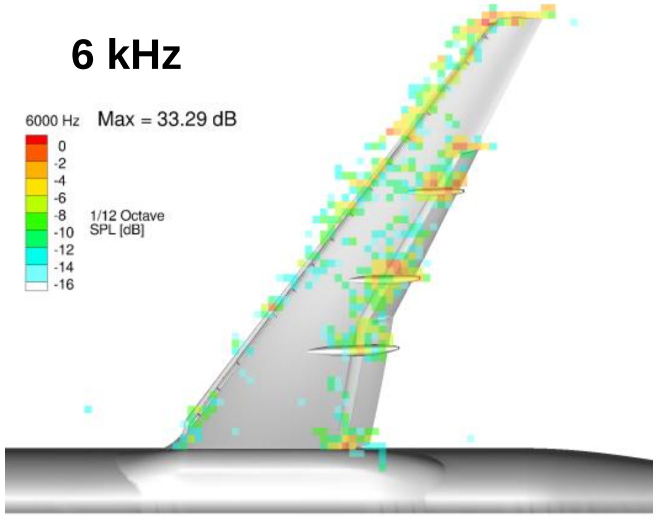

10 kHz

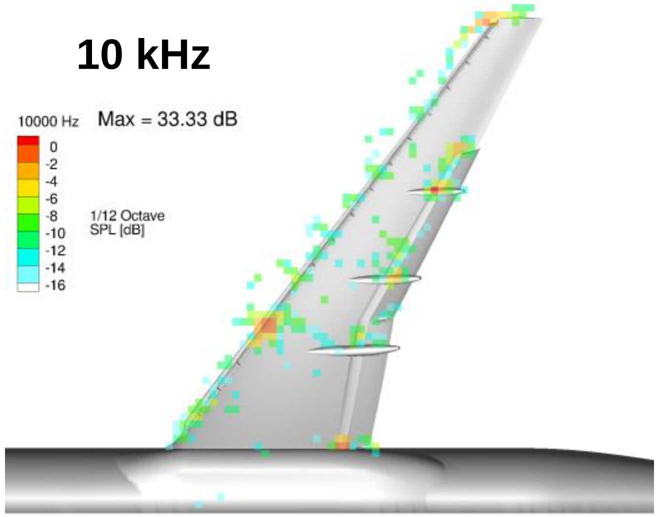

20 kHz

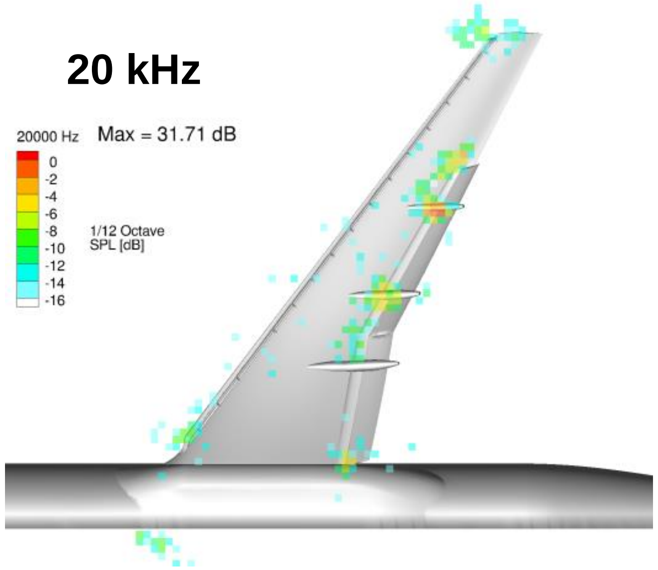

1/12-octave band MCF-DAMAS output, P3047
$\alpha = 8.5°$, $M = 0.16$, $\phi = 90°$

Slat Gap Filler FSS – Configuration 2

Comparison of Configurations 1/2

α = 8.5°, M = 0.16

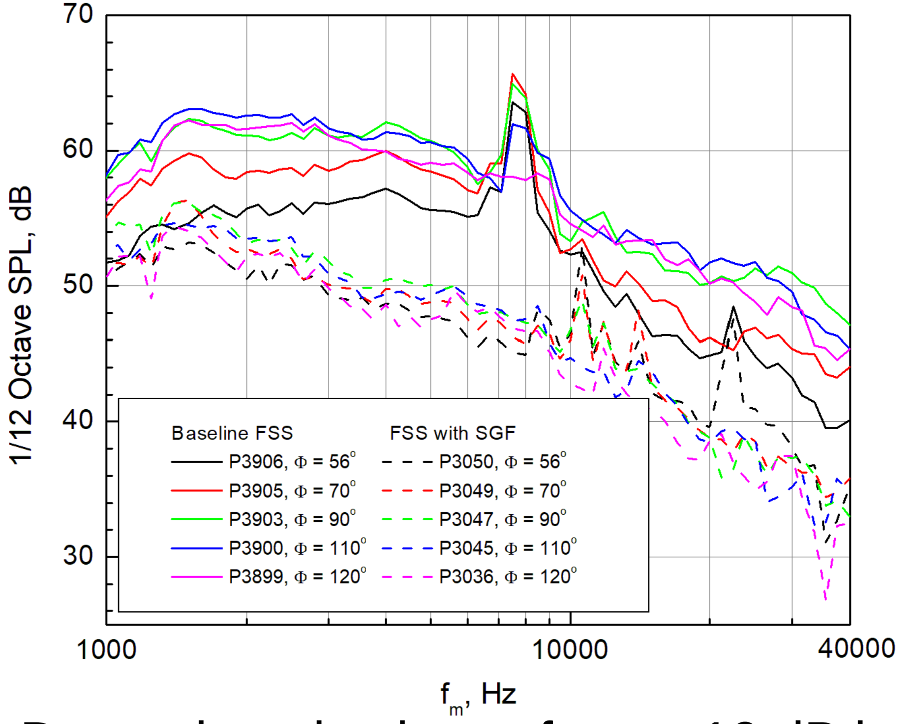

Mach Number Scaling

α = 8.5°, M = 0.16

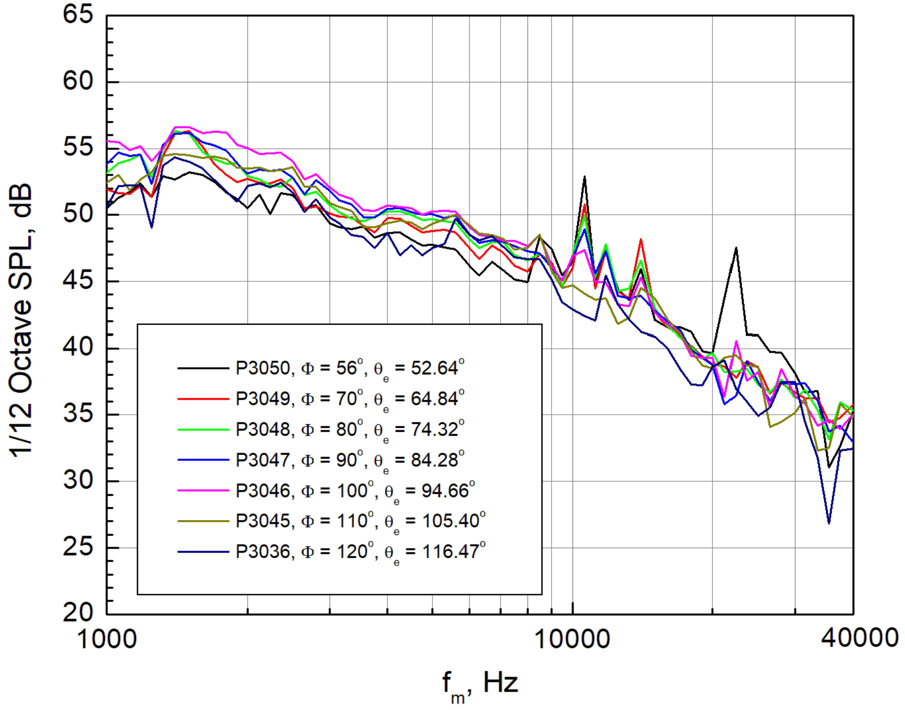

- Dramatic reductions of up to 10 dB in the spectral levels are observed with addition of SGF.
- Approximate dipole directivity observed for baseline FSS replaced with omnidirectional noise for FSS/SGF.
- Mach number scaling shows sixth power dependency on flow speed across entire frequency band.

CRM-HL Phased Array Testing - Takeaways

- Inclusion of SGF significantly reduced radiated noise along entire length of slat, typically by 10 dB.
- Flap noise not a significant contributor to overall radiated sound field.
- Directivity measurements revealed a rough dipole pattern for the baseline FSS noise. Incorporation of the SGF transitioned the radiated noise into an omnidirectional pattern.
- Observed Mach number scaling showed sixth power dependency on flow speed, although this only applied to higher frequencies for the baseline FSS.

Aeroacoustic Simulations of the High-Lift Common Research Model and Validation with Experiment

Lockard, D. P., Choudhari, M. M., and Vatsa, V. N.

Objectives

- Perform Powerflow numerical simulations of the CRM-HL
- Assess the simulations against experimental data

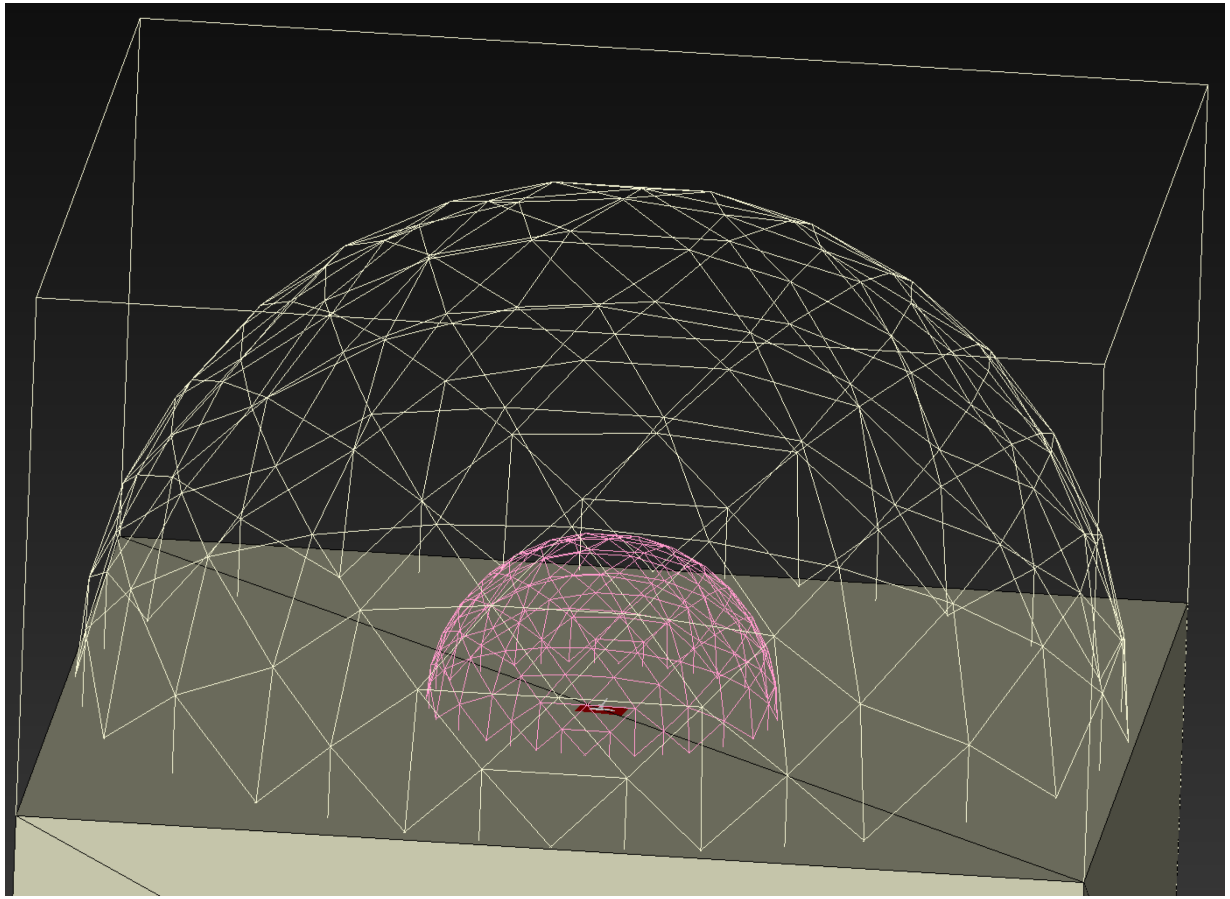

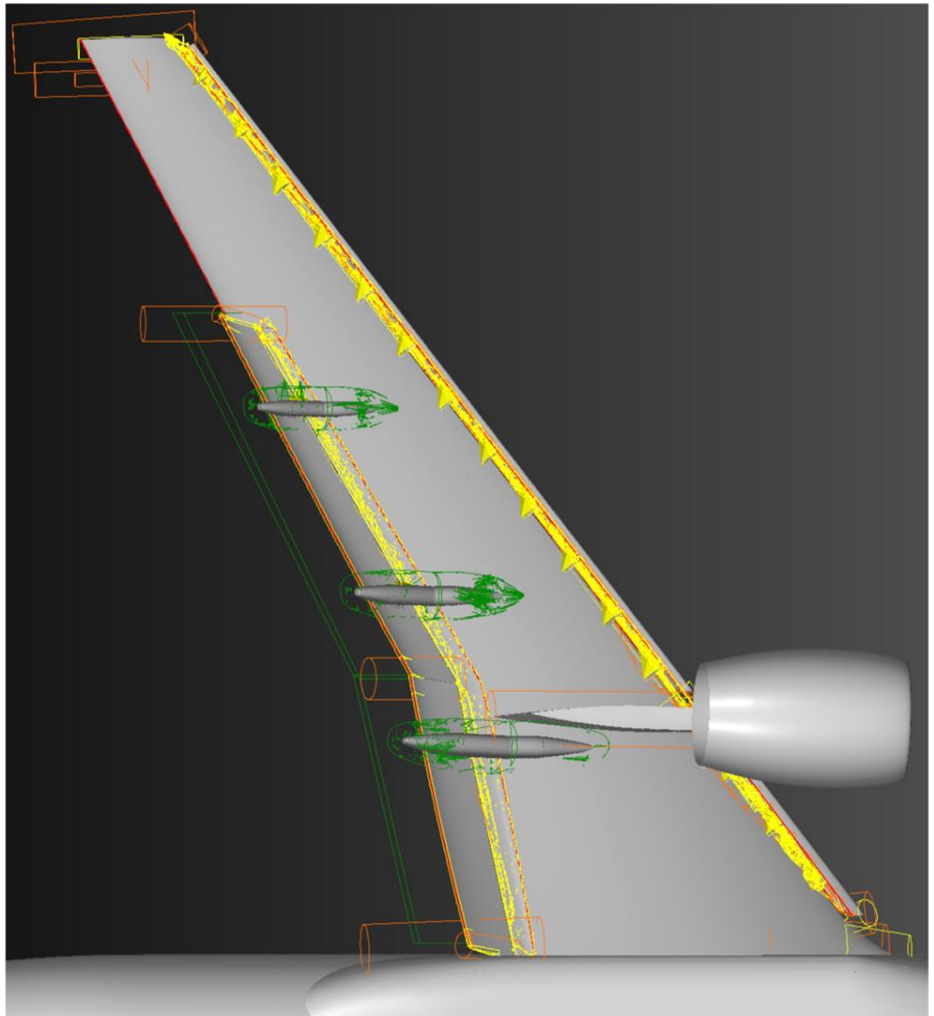

Steady Surface Pressure, PSS with SGF

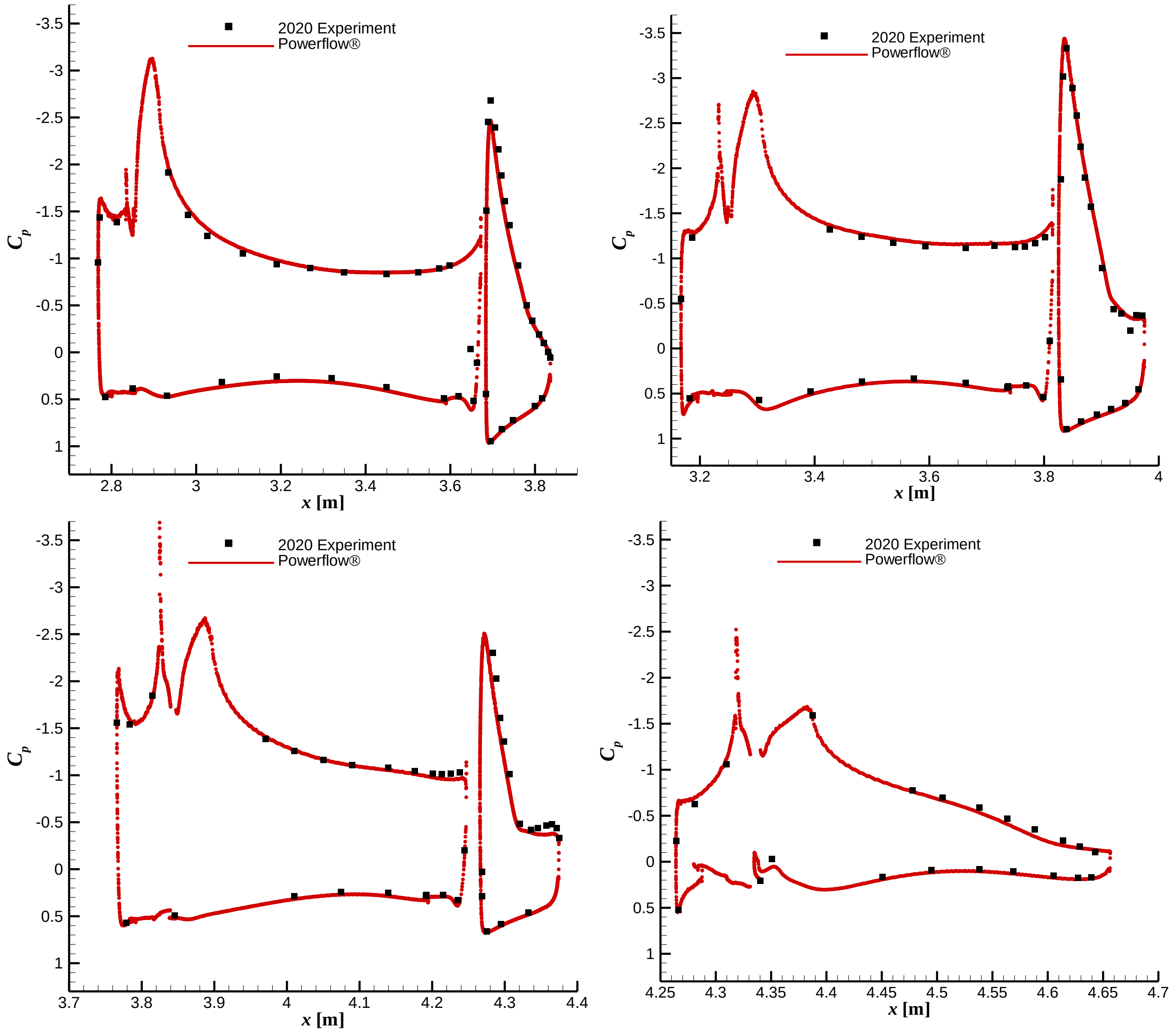

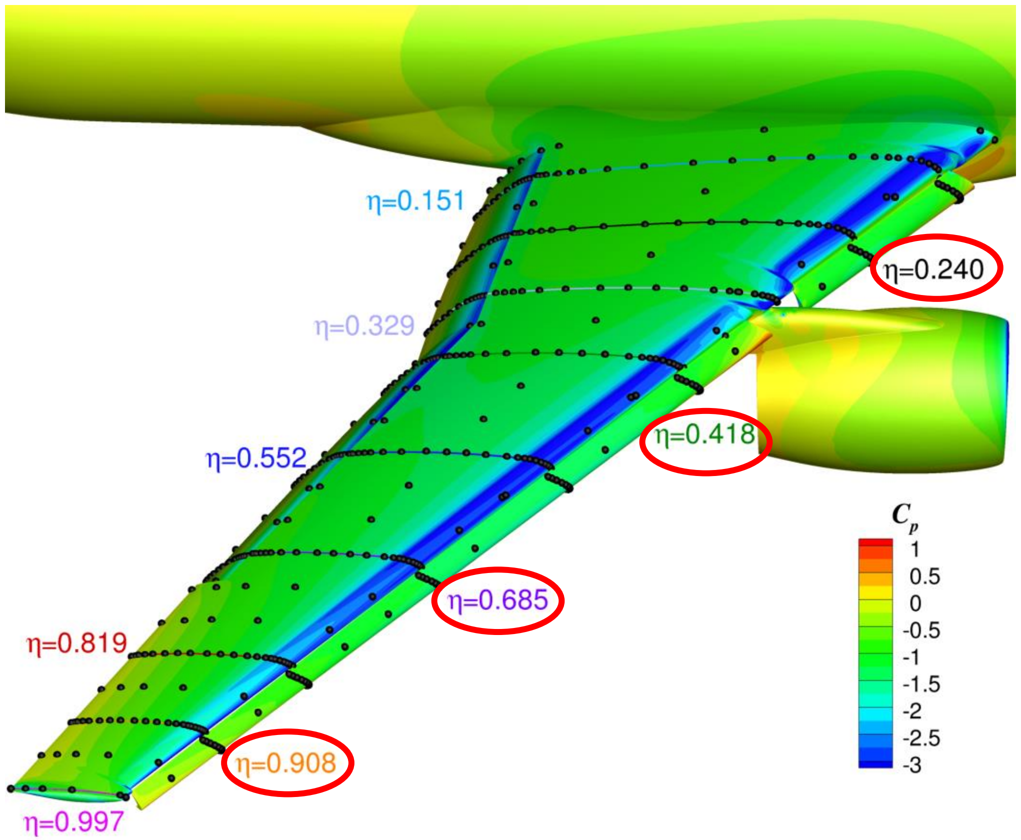

■ **2020 Experiment**

— **Powerflow Simulation**

AoA = 8.5°, M = 0.2

Unsteady Surface Pressure Spectra

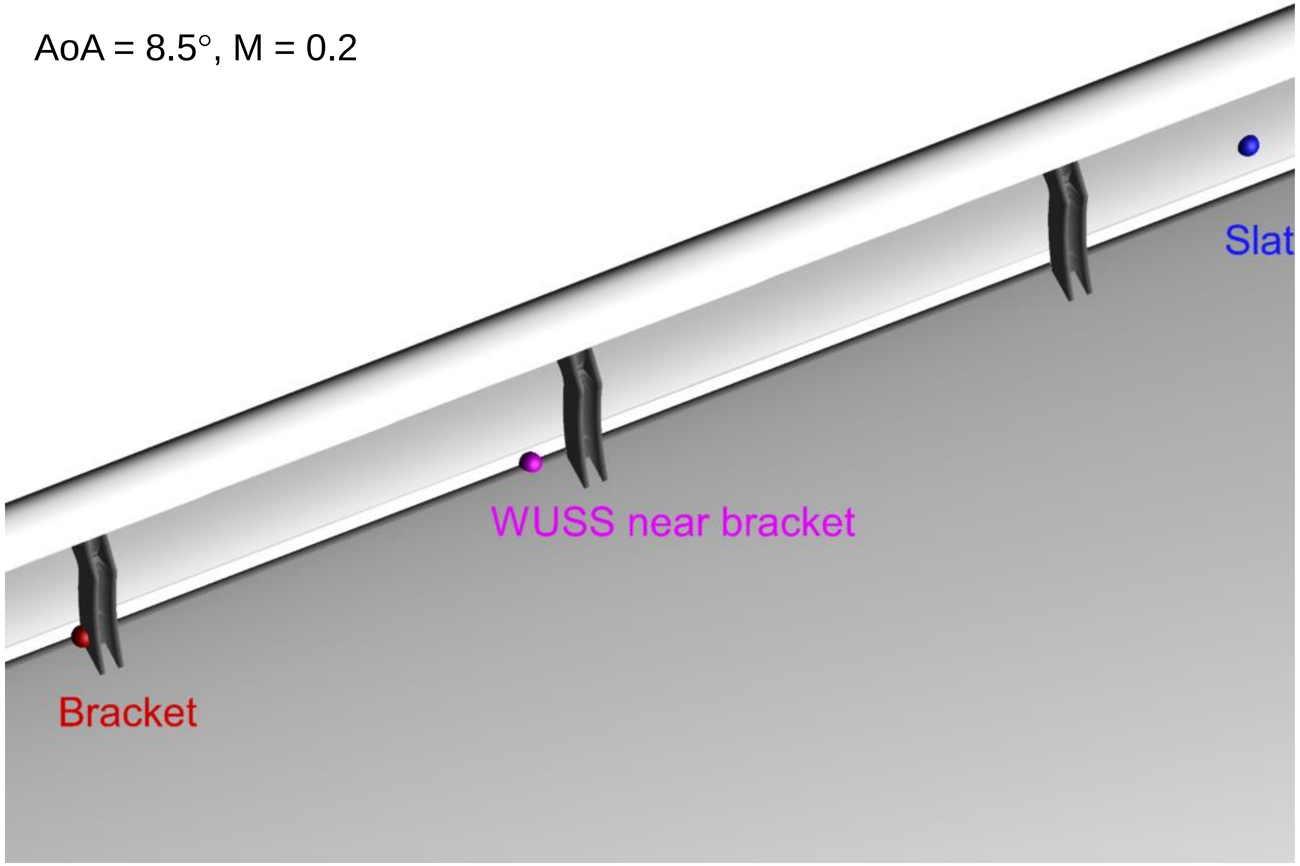

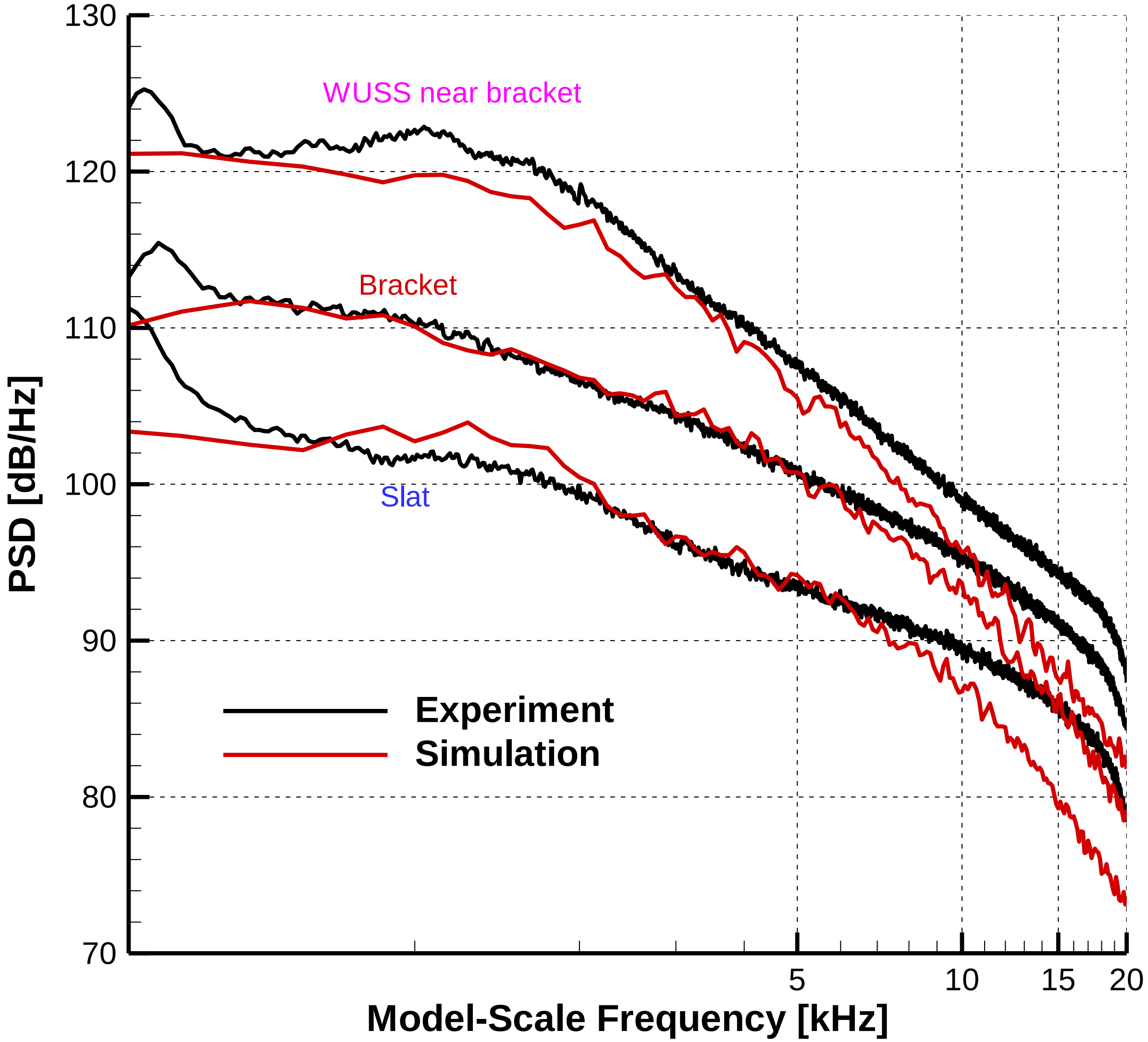

- **Good agreement at most points**
- **Highest levels are associated with the bracket wakes**

CRM-HL Simulations

- Good agreement between simulations and experiment for aerodynamic quantities
- Simulations provided valuable guidance during the development of the noise reduction treatments
- Noise predictions from the simulations reproduced the correct trends but had obvious errors
  - Permeable Ffowcs Williams-Hawkings data surfaces should have been used, but the calculations were cost prohibitive

Questions?